Influence of In_2O_3 capping and annealing on the luminescence properties of Ga_2O_3 nanorods

2012 Phys. Scr. 2012 014053

(http://iopscience.iop.org/1402-4896/2012/T149/014053)

Phys. Scr. **T149** (2012) 014053 (4pp) doi:10.1088/0031-8949/2012/T149/014053

Influence of In_2O_3 capping and annealing on the luminescence properties of Ga_2O_3 nanorods

Changhyun Jin[1], Sunghoon Park[1], Hyunsu Kim[1], Hyoun Woo Kim[2] and Chongmu Lee[1]

[1] Department of Materials Science and Engineering, Inha University, Yonghyeondong, Incheon 402-751, Korea

[2] Division of Materials Science and Engineering, Hanyang University, 17 Haengdang, Seongdong-gu, Seoul 133-791, Korea

E-mail: cmlee@inha.ac.kr

Received 25 August 2011
Accepted for publication 31 October 2011
Published 27 April 2012
Online at stacks.iop.org/PhysScr/T149/014053

Abstract

Ga_2O_3 nanorods were synthesized by thermal evaporation of GaN powders, and the influence of In_2O_3 capping and subsequent annealing on their luminescence properties was examined. The results of transmission electron microscopy and x-ray diffraction analyses indicated that the cores and shells of the annealed coaxial nanorods are monoclinic-structured single-crystal Ga_2O_3 and body-centered cubic-structured single-crystal In_2O_3, respectively. Photoluminescence (PL) measurements revealed that the blue emission band of Ga_2O_3 nanorods centered at approximately 460 nm was increased in intensity slightly by In_2O_3 coating and was increased in intensity further by subsequent thermal annealing. The PL peak was red-shifted from $\sim$ 460 to $\sim$ 530 nm by oxygen annealing. In contrast, the PL emission intensity of the nanorods was increased significantly and the PL peak was red-shifted from $\sim$ 460 to $\sim$ 590 nm by annealing in a reducing atmosphere. In addition, the origin of the PL intensity enhancement and of the PL peak shift by annealing is discussed.

PACS numbers: 61.46.−w, 78.55.Hx, 81.15.Gh

(Some figures may appear in colour only in the online journal)

1. Introduction

β-Ga_2O_3 is an important wide-band-gap semiconductor ($E_g \approx 4.9$ eV) with a monoclinic structure [1]. This material has potential applications in high-temperature gas sensors and optoelectronic devices owing to its conductive and luminescence properties [2]. Various forms of one-dimensional (1D) β-Ga_2O_3 nanostructures have been synthesized by a range of methods such as direct current (dc) arc discharge of GaN powders with a catalyst [3], thermal evaporation of Ga powders [4], thermal annealing of GaN powders [5], thermal annealing of GaAs in an oxygen atmosphere [3], thermal reaction of Ga_2O_3 powders with graphite of active carbon/carbon nanotubes [4], silica-assisted Fe catalytic growth [6], metal-organic chemical vapor deposition [7] and so on. In this paper, we chose the thermal evaporation technique of GaN powders for the synthesis of Ga_2O_3 nanorods because it is the technique easiest to control and offers 1D nanostructures with a relatively good quality.

In recent years, core–shell nanostructures have become the focus of intensive research owing to their potential applications in electronic, optoelectronic and biological applications. A variety of tailor-made functions can be obtained by fabricating core–shell nanostructures [8–10]. In this paper, the influence of In_2O_3 capping and subsequent annealing on the photoluminescence (PL) properties of Ga_2O_3 nanorods was examined in order to gain insight into how to tailor the optical properties of Ga_2O_3 nanorods [11–16]. The radio-frequency (RF) magnetron sputtering technique was employed to cap Ga_2O_3 nanorods with In_2O_3.

2. Experiment

Au-coated Si was used as a substrate for the synthesis of 1D Ga_2O_3 structures. Au was deposited on a (100) Si substrate by RF magnetron sputtering. A quartz tube was mounted horizontally inside a tube furnace. 99.99% pure GaN powders were placed on the lower holder at the center of the quartz tube. The Au-coated Si substrate was placed on the upper holder at approximately 5 mm distance from the GaN powders. The furnace was heated to 1050 °C and maintained at that temperature for 1 h in a N_2/3 mol% O_2 atmosphere with constant flow rates of oxygen (O_2) (15 sccm) and N_2 (485 sccm). The total pressure was set to 1.5 torr. Subsequently, the substrate was transferred to an RF magnetron sputtering system for In_2O_3 coating. The sputtering was performed at room temperature for 15 min using a 99.95% In_2O_3 target. The sputtering process parameters for In_2O_3 deposition used in the sputtering process are as follows: RF power = 100 W, base vacuum = 1.0×10^{-6} torr, chamber pressure = 1.8×10^{-2} torr, Ar gas flow rate = 30 sccm and substrate temperature = room temperature. After In_2O_3 coating, the products were annealed at 700 °C for 1 h in an O_2 or N_2/3 mol % H_2 atmosphere.

The morphologies of the prepared core–shell nanorod samples were examined by field emission scanning electron microscopy (FESEM; Hitachi S-4200). The microstructures and compositions of the nanorod samples were characterized further by a transmission electron microscope (TEM; Phillips CM-200) equipped with an energy dispersive x-ray (EDX) spectrometer. X-ray diffraction (XRD; Philips X'pert MRD) was performed using Cu K_α radiation to identify the morphology and structure of the nanorod samples. PL measurements were carried out at room temperature in a SPEC-1403 PL spectrometer with a He-Cd laser line of 325 nm as the excitation source (1 K, Kimon, Japan).

3. Results and discussion

Figure 1(a) shows the SEM image of the Ga_2O_3-core/In_2O_3-shell 1D nanostructures synthesized in our work. Most of the nanostructures had a rod-like morphology. The rod-like nanostructures are quite uniform in diameter. The nanorods were a few hundreds of nanometers in diameter and a few tens of micrometers in length. Each nanorod showed a globular particle at its tip with a diameter larger than that of the other part of it, as can be seen in the enlarged SEM image in the inset of figure 1(a). The EDX spectrum (figure 1(b)) taken from the tip of a typical core–shell nanorod indicates that the nanorod comprises Au as well as Ga, In and O. Such a growth feature suggests that the nanorods were likely formed by a vapor–liquid–solid mechanism.

XRD patterns of the as-synthesized core–shell nanorods are presented in figure 2. The main diffraction peaks in the pattern of the as-synthesized core–shell nanorods (figure 2) can be assigned to a monoclinic structure, in good agreement with the reported data of bulk β-Ga_2O_3 crystals (JCPDS card no. 43-1012, $a = 1.223$ nm, $b = 0.304$ nm, $c = 0.580$ nm, $\beta = 103.7°$), indicating that the nanomaterial is β-Ga_2O_3. In

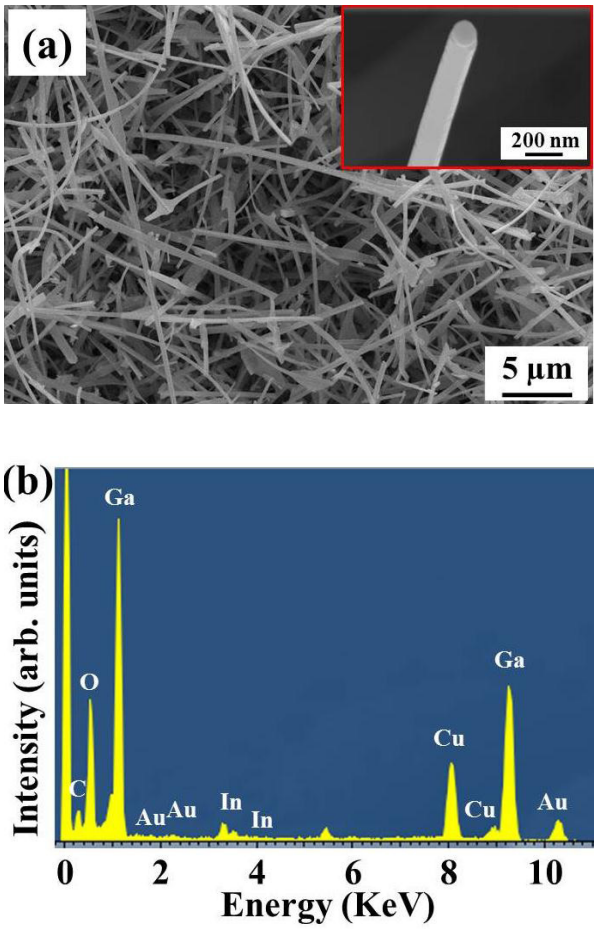

Figure 1. (a) SEM image of Ga_2O_3-core/In_2O_3-shell nanorods. Inset: enlarged SEM image of a typical nanorod showing a globular particle at its tip and (b) EDX spectra taken from the Ga_2O_3-core/In_2O_3-shell nanorod in the inset of figure 1(a).

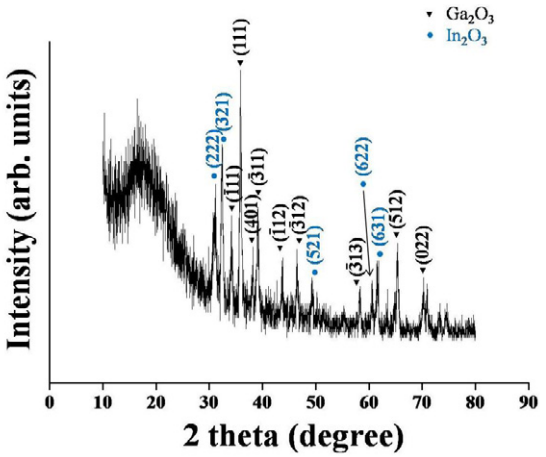

Figure 2. XRD patterns of annealed Ga_2O_3-core/In_2O_3-shell nanorods.

addition to nine reflections from Ga_2O_3, the reflections from the (222), (321), (521), (622) and (631) lattice planes of body-centered cubic (bcc)-structured In_2O_3 (JCPDS no. 06-0416; $a = 1.011$ nm) were identified, suggesting that In_2O_3 shells are also crystalline.

Figure 3(a) shows a local high-resolution TEM (HRTEM) image enlarging the core–shell interface region of a typical Ga_2O_3-core/In_2O_3-shell nanorod. The resolved spacing

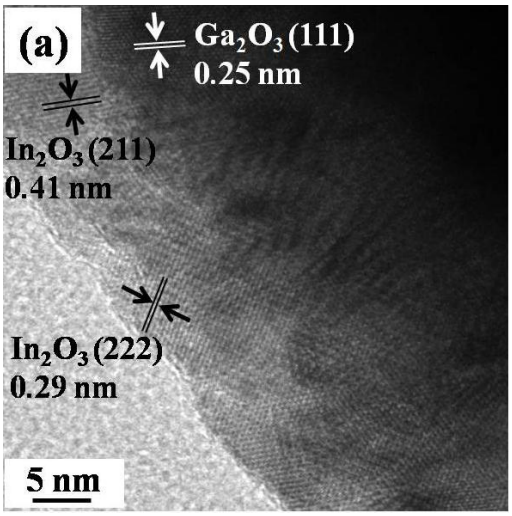

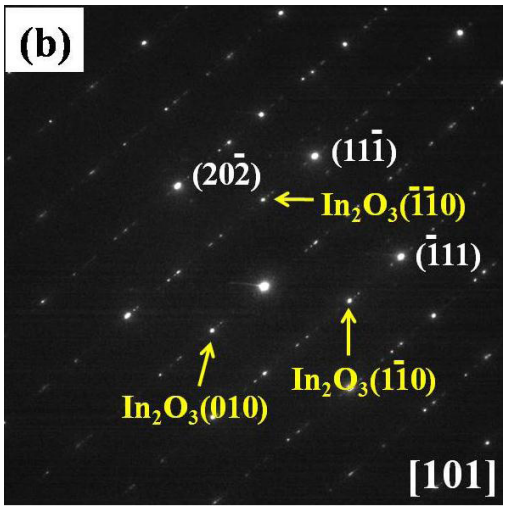

Figure 3. (a) Local HRTEM image of the nanostructure in the core–shell interface region. (b) The corresponding SAED pattern with the [101] zone axis of the nanomaterial in the same region as in the HRTEM.

between the two parallel neighboring fringes in the core region was approximately 0.25 nm, corresponding to the monoclinic β-Ga_2O_3 (111) plane, whereas those between the two parallel neighboring fringes in the shell region were 0.41 and 0.29 nm, corresponding to bcc In_2O_3 (211) and (222), respectively. The corresponding selected area electron diffraction (SAED) pattern (figure 3) recorded perpendicular to the long axis of the nanorod is to the [101] crystal zone of β-Ga_2O_3. Not only the TEM image but also the SAED pattern verifies that the core is monoclinic-structured single-crystal β-Ga_2O_3 and that the shell is bcc-structured single-crystal In_2O_3.

Figure 4 displays the PL spectra, measured at room temperature, of the Ga_2O_3-core/In_2O_3-shell nanorods annealed in different annealing atmospheres along with as-synthesized Ga_2O_3 nanorods and Ga_2O_3-core/In_2O_3-shell nanorods. The as-synthesized Ga_2O_3 nanorods showed an emission band centered at approximately 460 nm in the blue region. This blue emission is in good agreement with previous reports and is assumed to be associated with the vacancies in Ga_2O_3 nanorods, such as gallium (Ga) vacancies,

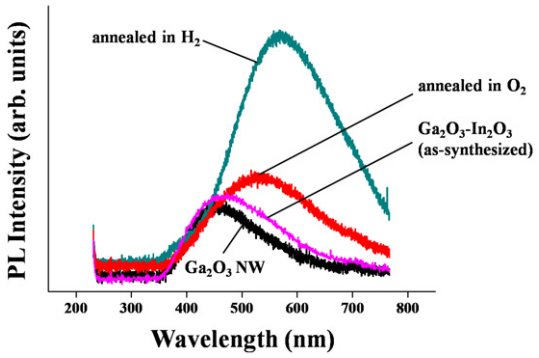

Figure 4. Room temperature PL spectra of the Ga_2O_3-core/In_2O_3-shell nanorods annealed at 700 °C for 1 h at different atmospheres along with as-synthesized Ga_2O_3 and Ga_2O_3-core/In_2O_3-shell nanorods.

oxygen (O) vacancies [17] and Ga–O vacancy pairs [18] according to previous reports. Binet and Gourier [19] observed blue emission from Ga_2O_3 nanowires previously. They reported that this emission might be produced by the tunnel recombination of an electron on a donor with a hole on an acceptor, which could be either a Ga vacancy (V_{Ga}) or a charged Ga or O vacancy. Vacancies might have been easily generated, as the Ga_2O_3 nanorods were synthesized by thermal evaporation of GaN powders at a temperature as high as 1050 °C. On the other hand, the intensity of the blue emission from Ga_2O_3 nanorods was increased slightly but the PL peak was not shifted by coating them with In_2O_3. The blue emission from the Ga_2O_3-core/In_2O_3-shell nanorods probably originates not from the In_2O_3 shells but from the Ga_2O_3 cores, because the shell layers are much thinner than the cores even though the blue emission from In_2O_3 nanostructures has been reported previously. Regarding the PL properties of In_2O_3 nanostructures, it is well known that bulk In_2O_3 cannot emit light at room temperature [20]. However, Zhou *et al* observed PL peaks at 480 and 520 nm from the In_2O_3 nanoparticles [21]. Lee *et al* noticed a peak at 637 nm for In_2O_3 films [22]. Liang *et al* observed a peak at 470 nm from In_2O_3 nanofibers [23] and recently Wu *et al* reported two distinct peaks at 416 and 435 nm for In_2O_3 nanowires [24]. These emissions are commonly referred to as deep level emissions due to oxygen deficiencies.

The major emission intensity of the Ga_2O_3-core/In_2O_3-shell nanorods was increased further and the emission peak was shifted from ∼460 nm (the blue region) to ∼530 nm (the green region) by subsequent thermal annealing in an O_2 atmosphere. In contrast, the emission intensity was significantly enhanced and the emission peak was shifted from ∼460 to ∼590 nm (the yellow region) by thermal annealing in a N_2/3 mol % H_2 atmosphere. The O concentration in the Ga_2O_3 core region might be decreased by N_2/3 mol % H_2 annealing. The decrease in the oxygen (O) concentration in the cores, in turn, may have led to an increase in the O vacancies, resulting in the enhancement of the blue emission. It is well known that oxygen vacancies are generated in Ga_2O_3 under reduced growth conditions, forming an n-type semiconductor. Harwig and Kellendonk [17] showed that samples annealed in a reducing atmosphere were in favor of the formation of O vacancies and the blue emission was enhanced, while samples heated in an O_2 atmosphere were

in favor of the formation of Ga vacancies, which showed a dominant green emission.

Another source of the enhancement in PL intensity and the red-shift of the major emission band by annealing in a reducing atmosphere might be the radiative recombination of self-trapped excitations by diffusion of indium (In) atoms from the shell to the core during the annealing process. It appears that the Ga_2O_3 cores and In_2O_3 shells were not dissociated spontaneously by reacting with hydrogen during the annealing process at 700 °C in a reducing atmosphere as can be seen from the Gibbs free-energy change values in the following equations [25]:

$$\mathrm{Ga_2O_3(s) + 3H_2(g) = 2Ga(l) + 3H_2O(g)} \uparrow \Delta G_{\mathrm{f,973\,K}} = 188.589\,\mathrm{J\,mol^{-1}}, \quad (1)$$

$$\mathrm{In_2O_3(s) + 3H_2(g) = 2\,In\,(l) + 3H_2O\,(g)} \uparrow \Delta G_{\mathrm{f,973\,K}} = 29.611\,\mathrm{kJ\,mol^{-1}}. \quad (2)$$

However, the as-deposited In_2O_3 films are commonly known to be In-rich. Therefore, it is likely that the extra In atoms in the In_2O_3 layer diffused into the Ga_2O_3 core at the annealing temperature of 700 °C. Consequently, the In impurity concentration in the core might have increased, which also presumably made a contribution to the enhancement in PL intensity.

4. Conclusions

Ga_2O_3-core/In_2O_3-shell nanorods were prepared by a two-step process: thermal evaporation of GaN powders and sputter deposition of In_2O_3. The cores and shells were monoclinic-structured single-crystal Ga_2O_3 and bcc-structured single-crystal In_2O_3, respectively. The intensity of the blue emission from Ga_2O_3 nanorods was increased slightly by In_2O_3 coating. The major emission peak was shifted from 460 to 530 nm and its intensity was increased further by subsequent thermal annealing in an oxidizing atmosphere. In contrast, the emission major peak was red-shifted from 460 to ∼ 590 nm and its intensity was increased significantly by annealing in a reducing atmosphere, which was presumably caused by increases in the O vacancy and In interstitial concentrations in Ga_2O_3 nanorods. The results obtained in this study give insight into tailoring the optical properties of semiconductor nanostructures by means of capping and thermal annealing.

Acknowledgment

This work was financially supported by an Inha University research grant.

References

[1] Tippins H H 1965 Optical absorption and photoconductivity in the band edge of β-Ga_2O_3 *Phys. Rev.* **140** A316–9
[2] Yamazoe N 1991 New approaches for improving semiconductor gas sensors *Sensors Actuators* B **5** 7–19
[3] Gundiah G, Govindaraj A and Rao C N R 2002 Nanowires, nanobelts and related nanostructures of Ga_2O_3 *Chem. Phys. Lett.* **351** 189–94
[4] Zhang H Z, Kong Y C, Wang Y Z, Du X, Bai Z G, Wang J J, Yu D P, Ding Y, Hang Q L and Feng S Q 1999 Ga_2O_3 nanowires prepared by physical evaporation *Solid State Commun.* **109** 677–82
[5] Kim B C, Sun K T, Park K S, Im K J, Noh T, Sung M Y, Kim S, Nahm S, Choi Y N and Park S S 2002 β-Ga_2O_3 nanowires synthesized from milled GaN powders *Appl. Phys. Lett.* **80** 479–81
[6] Gao Y H, Bando Y, Sato T, Zhang Y F and Gao X Q 2002 Synthesis, Raman scattering and defects of β-Ga_2O_3 nanorods *Appl. Phys. Lett.* **81** 2267–9
[7] Tang C C, Fan S S, de la Chapelle M L and Li P 2001 Silica-assisted catalytic growth of oxide and nitride nanowires *Chem. Phys. Lett.* **333** 12–5
[8] Sanchez-Castillo M A, Couto C, Kim W B and Dumesic J A 2004 Gold-nanotube membrane for the oxidation of CO at gas–water interfaces *Angew. Chem.* **116** 1160–2
[9] Jágerszki G, Gyurcsányi R E, Höefler L and Pretsch E 2007 Hybridization-modulated ion fluxes through peptide-nucleic-acid-functionalized gold nanotubes. A new approach to quantitative label-free DNA analysis *Nano Lett.* **7** 1609–12
[10] Oshima Y and Onga A 2003 Helical gold nanotube synthesized at 150 K *Phys. Rev. Lett.* **91** 205503
[11] Lauhon L J, Gudiksen M S, Wang D and Lieber C M 2002 Epitaxial core–shell and core–multishell nanowire heterostructures *Nature* **420** 57–61
[12] Tang C C, Bando Y, Sato T and Kurashima K 2002 Uniform boron nitride coatings on silicon carbide nanowires *Adv. Mater.* **14** 1046–9
[13] Han W and Zettl A 2002 An efficient route to graphitic carbon layer coated gallium nitride nanorods *Adv. Mater.* **14** 1560–2
[14] Kim H W, Shim S H and Lee C 2007 Effects of thermal annealing on the properties of ZnO-coated MgO nanowires *Mater. Sci. Eng.* B **136** 148–53
[15] Park S, Kim H, Lee J W, Kim H W and Lee C 2008 Influence of a ZnO coating on the photoluminescence properties of SnO_2 nanobelts *J. Korean Phys. Soc.* **53** 657–61
[16] Jun J, Jin C, Kim H, Kang J and Lee C 2009 The structure and photoluminescence properties of TiO_2-coated ZnS nanowires *Appl. Phys.* A **96** 813–8
[17] Harwig T and Kellendonk F 1978 Some observations of the photoluminescence of doped β-gallium sesquioxide *J. Solid State Chem.* **24** 255–63
[18] Vasiltsiv V, Zakharko Y M and Rym Y M 1988 On the nature of blue and green luminescence bands of β-Ga_2O_3 *Ukr. Fiz. Zh.* **33** 1320–4
[19] Binet L and Gourier D 1995 Origin of the blue luminescence of β-Ga_2O_3 *J. Phys. Chem. Solids* **59** 1241–9
[20] Wu X C, Hong J M, Han Z J and Tao Y R 2003 Fabrication and photoluminescence characteristics of single crystalline In_2O_3 nanowires *Chem. Phys. Lett.* **373** 28–32
[21] Zhou H, Cai W and Zhang L 1999 Photoluminescence of indium-oxide nanoparticles dispersed within pores of mesoporous silica *Appl. Phys. Lett.* **75** 495–7
[22] Lee M-S, Choi W C, Kim E K, Kim C K and Min S-K 1996 Characterization of the oxidized indium thin films with thermal oxidation *Thin Solid Films* **279** 1–3
[23] Liang C H, Meng G W, Lei Y, Phillipp F and Zhang L D 2001 Catalytic growth of semiconducting In_2O_3 nanofibers *Adv. Mater.* **13** 1330–3
[24] Guha P, Kar S and Chaudhuri S 2004 Direct synthesis of single crystalline In_2O_3 nanopyramids and nanocolumns and their photoluminescence properties *Appl. Phys. Lett.* **85** 3851–3
[25] Barin I 1995 *Thermochemical Data of Pure Substances* 3rd edn (Weinheim: VCH)